Available online at www.sciencedirect.com
ScienceDirect
Trans. Nonferrous Met. Soc. China 25(2015) 3223−3231
Transactions of Nonferrous Metals Society of China
www.tnmsc.cn

Effects of Nd and rotary forging on mechanical properties of AZ71 Mg alloys

Jhewn-kuang CHEN[1], Yu-cheng CHEN[1], Hsien-tsung LI[2], Kam-shau CHAN[2], Chun-jung CHANG[2]

1. Institute of Materials Science and Engineering, National Taipei University of Technology, Taipei 10608;
2. Foxconn Technology Group, New Taipei 23680

Received 21 November 2014; accepted 18 March 2015

Abstract: The effects of Nd addition on the mechanical properties and plastic deformability of AZ71 Mg alloys were investigated. 0.5%−2.0% (mass fraction) Nd was added to AZ71 Mg alloys. The grain size and the amount of brittle β-$Mg_{17}Al_{12}$ phase reduce with increasing the Nd addition, while nanosized Al_xNd_y precipitates form. In combination with 32% rotary forging and subsequent annealing, the grain size of Nd-added AZ71 Mg alloys reduces greatly from over 350 μm to below 30 μm. Both tensile strength and ductility increase with the Nd addition up to 1.0%. The addition of Nd beyond 1.0% leads to the aggregations of rod-shaped $Al_{11}Nd_3$ and blocky Al_2Nd precipitates, thereby deteriorating both strength and ductility. The 1.0% Nd-added AZ71 Mg alloy shows tensile strength up to 253 MPa and elongation of 10.7%. It is concluded that adding 1.0% Nd to AZ71 Mg alloy yields the optimum toughness, whether under as-cast or rotary forging and annealing conditions.

Key words: AZ71 Mg alloys; Nd; rotary forging; mechanical properties; recrystallization

1 Introduction

Mg alloy, renowned as the 21st century green engineering material, has emerged as the third metallic structural material, following steels and Al alloys [1−3]. Despite increasing emphasis on energy conservation and environmental issues, development and application of Mg and Mg alloys are still limited due to the following concerns. 1) Mg alloys have few slip systems and usually have poor ductility and thus inferior forming ability. Furthermore, the formation of brittle β-$Mg_{17}Al_{12}$ phase largely impairs their ductility [4]. 2) The difference in corrosion potentials of α-Mg and β-$Mg_{17}Al_{12}$ phases causes severe galvanic corrosion and poor corrosion resistance properties of Mg alloys. 3) The low melting point of β-$Mg_{17}Al_{12}$ phase tends to soften the Mg alloys and demonstrates poor high temperature properties.

Two routes were employed to resolve the above-mentioned issues in Mg alloys. Firstly, ZHANG et al [5] proposed to refine grain size to below 10 μm by combining severe plastic deformation (SPD) and heat treatment. The fine grain size can give rise to superplastic properties at high temperature, leading to significant enhancement of high-temperature forming ability. AZ61 Mg alloy was shown to produce grains with size of 3.5 μm via repetitive upsetting−extrusion process [6]. CHAPMAN and WILSON [7] showed that when the grain size is smaller than 2 μm, the ductile−brittle transition temperature of Mg alloys reduces to room temperature, thereby enhancing forming ability for cold forging. Secondly, by the addition of strengthening elements, intermetallic compounds with high melting point can form to improve mechanical properties of Mg alloys at both room and high temperatures [8,9]. And by eliminating the formation of β-$Mg_{17}Al_{12}$ phase, the corrosion resistance of Mg alloys can also be improved.

The present study chooses a less studied AZ71 Mg alloy with medium combination of strength and ductility compared with the deformable AZ31 and the high strength AZ91 Mg alloys. Two routes are pursued to improve the properties of AZ71 Mg alloy: adding neodymium (Nd) and plastic deformation using rotary forging. Nd is selected since its electronegativity (1.14) is closer to that of Mg (1.31) [10] than that of Al (1.61). This gives rise to higher Nd solid solubility in Mg than Al. It can also reduce the formation of β-$Mg_{17}Al_{12}$ phase [11]. On the other hand, Nd has been reported to have great effect on the grain refinement in Mg−4Al [12] and AZ80 Mg alloys [13], which improves both strength and ductility. The Nd-containing Mg alloys also showed improved high temperature deformability [14].

The current study uses rotary forging as the plastic deformation to assist grain size reduction, which has

Corresponding author: Jhewn-kuang CHEN; E-mail: jkchen@ntut.edu.tw
DOI: 10.1016/S1003-6326(15)63955-3

been employed for forming axis-symmetric products under plane stress in industrial production [15]. Although the strain of rotary forging process is lower than that of SPDs, the rotary forging process is nevertheless an industrial process that gives rise to reasonable magnitude of strain at a high strain rate [16]. It has also been reported recently that the rotary forging refined grains significantly in Al−15%Si composites [17] and reduced porosity in the work pieces, giving rise to fully dense materials [18]. Because the effects of rotary forging on Mg alloys are seldom reported and the porosity causes large property deviation in Mg die-castings [19]. The current study examines the effects of rotary forging on both the grain refinement and mechanical properties of 0−2% (mass fraction) Nd-added AZ71 Mg alloys.

2 Experimental

The materials were prepared by melting appropriate amount of Mg−20%Nd (mass fraction) master alloys and AZ71 Mg alloys to obtain 0−2% Nd (mass fraction) containing AZ71 Mg alloys. Melting was performed using an electrical furnace with CO_2+Ar protection and the melt was gravity cast at 700 °C into a Cu mould. The compositions of all alloys were analyzed using inductively coupled plasma method and are listed in Table 1.

Table 1 Compositions of Nd-added AZ71 alloys (mass fraction, %)

Alloy	Al	Zn	Mn	Si	Nd	Mg
AZ71	7.69	0.54	0.18	0.054	−	Bal.
AZ71+0.5%Nd	7.54	0.55	0.17	0.052	0.62	Bal.
AZ71+1%Nd	7.66	0.53	0.16	0.051	1.07	Bal.
AZ71+1.5%Nd	7.48	0.55	0.17	0.053	1.43	Bal.
AZ71+2%Nd	7.67	0.55	0.17	0.049	2.05	Bal.

The Nd-added AZ71 Mg alloys were then heated to 300, 380 and 420 °C under 1.33 Pa vacuum for 6 h before quenching into water to select an optimum homogenization temperature, so the 427 °C eutectic point in the Al−Mg phase diagram was not exceeded. One optimum homogenization temperature was selected based on the dissolution of dendrites formed in as-cast materials.

The homogenized Nd-added AZ71 Mg alloy rods were rotary forged with an engineering strain of 32% from 14.5 to 12 mm in diameter at a strain rate of 3 s^{-1} after heating at 200 °C for 15 min. The 32% strain was chosen so that the specimens did not fracture during the forging processes. The rotary forged specimens were then subjected to annealing at 200, 250, 300, and 350 °C under 1.33 Pa vacuum for 1 h. The optimal annealing processes for complete recrystallization were chosen to measure the mechanical properties of the annealed materials.

The microstructures of the as-cast, as-forged, and annealed Nd-added AZ71 Mg alloys were analyzed by optical microscopy, scanning electron microscopy (SEM, Hitachi S−4700), and transmission electron microscopy (FEI Tecnai F20). The chemical compositions of precipitates were analyzed using an energy dispersive X-ray spectroscopy (EDS) detector attached to the SEM. The quantitative measurements of precipitate were made on a Nikon Eclipse LV−150 optical microscope using an image processing software (Image-Pro Plus 6.0). The tensile tests were conducted using a Tinius Olsen universal tensile test machine at room temperature. The tensile specimens were prepared according to the small-size round tension test specimen 4 of ASTM E8/E8M standard [20].

3 Results and discussion

3.1 As-cast and homogenized structures

Figure 1 shows that the Nd-added AZ71 Mg alloys mainly consist of two phases: α-Mg (the matrix) and β-$Mg_{17}Al_{12}$ (the dark area). The as-cast grain sizes for Nd-added AZ71 Mg alloys obtained using the Jeffries Planimetric method are shown in Fig. 2. The as-cast grain size reduces with increasing the Nd addition up to 1.0%. The grain size does not decrease much when over 1.0% Nd is added.

According to the Mg−Al phase diagram, the Al-deficient primary α-Mg phase first forms during solidification. The residual liquid concentrates with Al residing in the dendrite arms and then transforms to primary β-$Mg_{17}Al_{12}$ precipitate and α-Mg+β-$Mg_{17}Al_{12}$ eutectic phases (Fig. 3).

The EDS analyses (Fig. 4) further show that, in Nd-added AZ71 Mg alloy, both faceted shaped Al_2Nd and $Al_{11}Nd_3$ rods form inside the α-Mg phase (Figs. 4(c) and (d)). The Al_2Nd and $Al_{11}Nd_3$ precipitates are confirmed by the selected area diffraction conforming with their corresponding crystal structures (Fig. 5). The observations of precipitates are consistent with those reported by WANG et al [13] in Nd-added AZ80 Mg alloys. In Fig. 5(b), nanosized Al_xNd_y precipitates with rod shape are also observed inside the α-Mg grains. Because the electronegativity of Mg is 1.31, that of Al is 1.61, and that of Nd is 1.14, the greater difference between the electronegativity of Al and Nd tends to form Al_xNd_y in preference to the β-$Mg_{17}Al_{12}$ phase [12,21]. The formation of Al_xNd_y indicates that Nd has a tendency of reacting with Al in the melt at high temperatures during solidification. More Al atoms are consumed by the Al_xNd_y phase, thereby reducing the

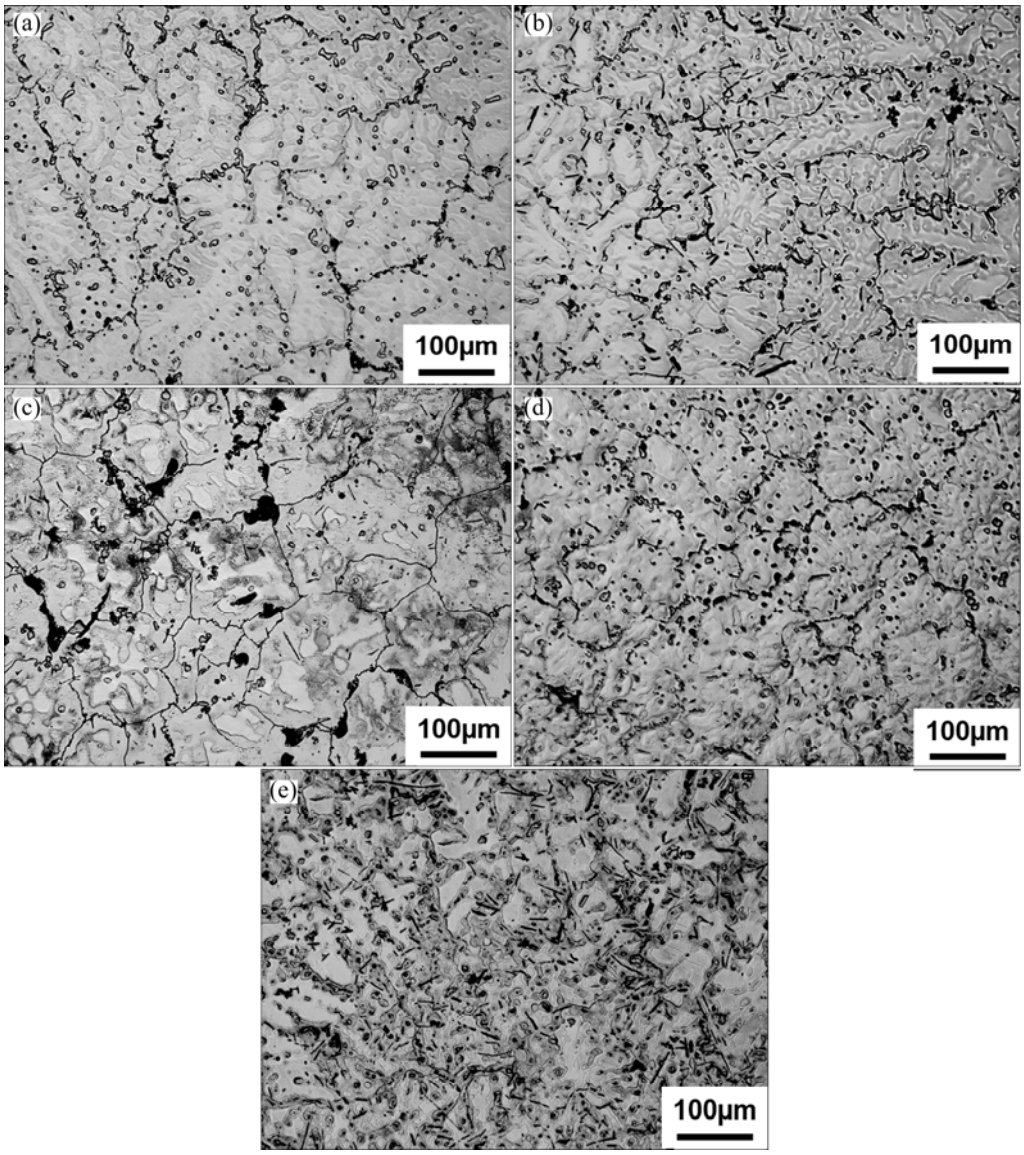

Fig. 1 As-cast microstructures of AZ71 alloy with different Nd additions: (a) 0; (b) 0.5%; (c) 1.0%; (d) 1.5%; (e) 2.0%

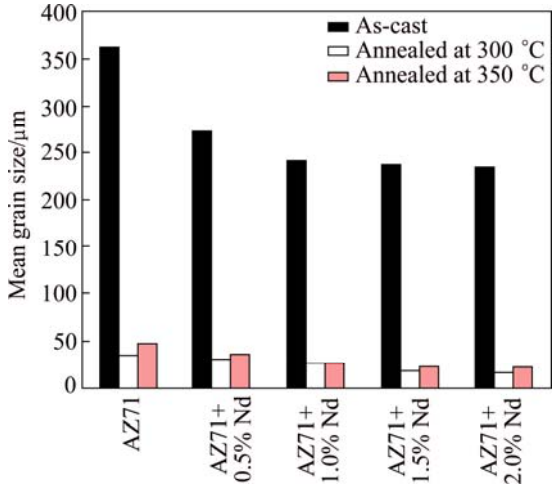

Fig. 2 Grain size of Nd-added AZ71 Mg alloys in as-cast state and with 32% rotary forging followed by annealing at 300 °C and 350 °C for 1 h

amount of Al in the liquid phase and suppressing the formation of β-$Mg_{17}Al_{12}$ eutectic phase at later stages of solidification. On the other hand, as low as 0.4% Nd was reported to enhance the α-Mg nucleation in AZ91 Mg alloy by reducing the solid−liquid interfacial energy causing the microstructure to refine [22]. Therefore, both the dissolved Nd atoms in the matrix and nanosized Al_xNd_y precipitates play a role in the grain size reduction.

The volume fraction of Al_xNd_y precipitates increases with increasing the Nd addition (Fig. 6). Small equiaxed Al_2Nd appears in the AZ71+0.5%Nd specimen. The addition of Nd over 1.0% increases the precipitation of $Al_{11}Nd_3$ which has fine rod shape. The rod-shaped $Al_{11}Nd_3$ precipitate is more enriched with Al than Al_2Nd. Figure 7 shows that both the volume fraction of Al_xNd_y precipitates and its deviation increase with increasing the Nd addition. The increase of standard deviation suggests that the Al_xNd_y precipitates tend to distribute

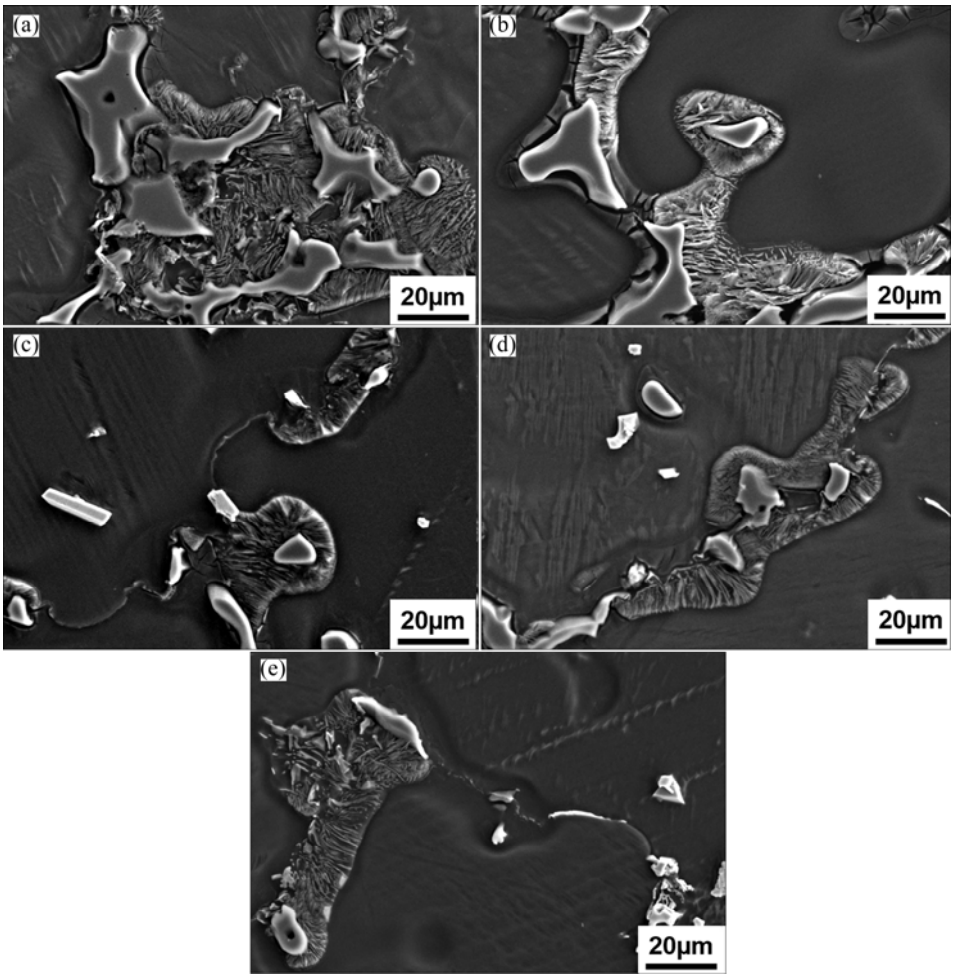

Fig. 3 Reduction of proeutectic β-$Mg_{17}Al_{12}$ and eutectic phases in as-cast Nd-added AZ71 Mg alloys with increasing Nd additions: (a) 0; (b) 0.5%; (c) 1.0%; (d) 1.5%; (e) 2.0%

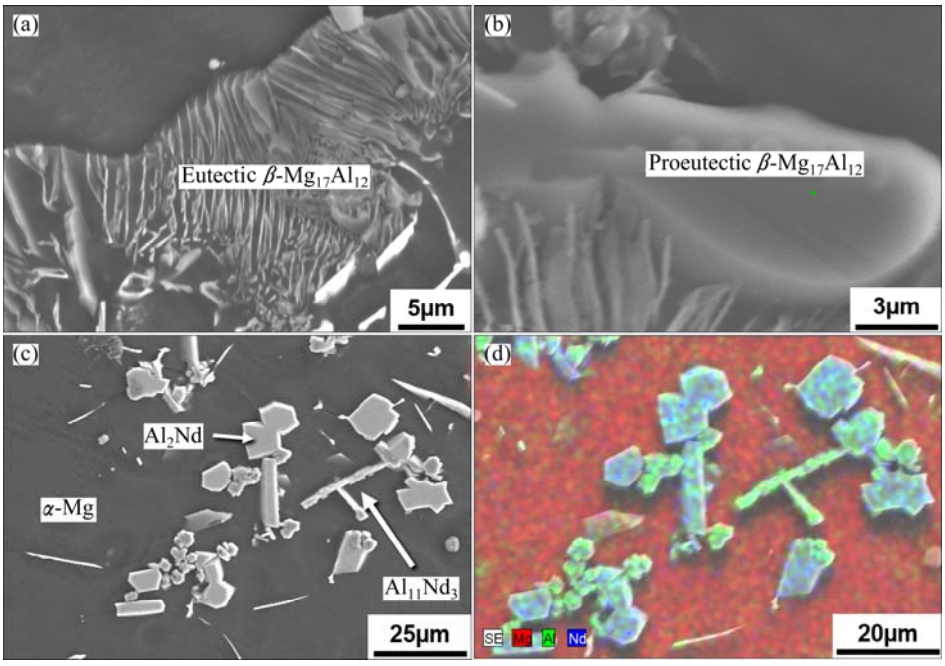

Fig. 4 EDS analyses of precipitates in as-cast AZ71 Mg alloy containing 2.0% Nd: (a) Eutectic phases; (b) Proeutectic β-$Mg_{17}Al_{12}$ phase; (c) Al_2Nd and $Al_{11}Nd_3$ phases; (d) Elemental mapping of (c)

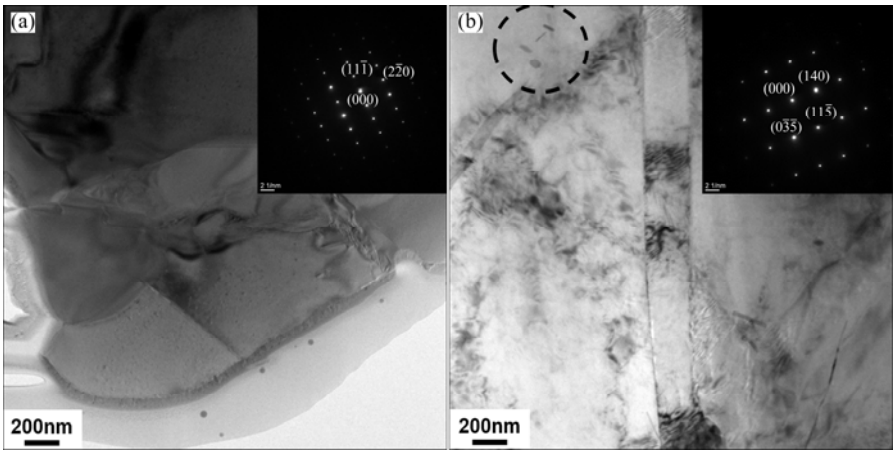

Fig. 5 Selected area diffraction patterns of $\langle 112\rangle Al_2Nd$ (a) and $\langle 20\bar{5}3\rangle$ $Al_{11}Nd_3$ (b) phases in as-cast AZ71 Mg alloy containing 2.0% Nd (Nanosized precipitates in α-Mg grains are indicated by circle in Fig. 5(b))

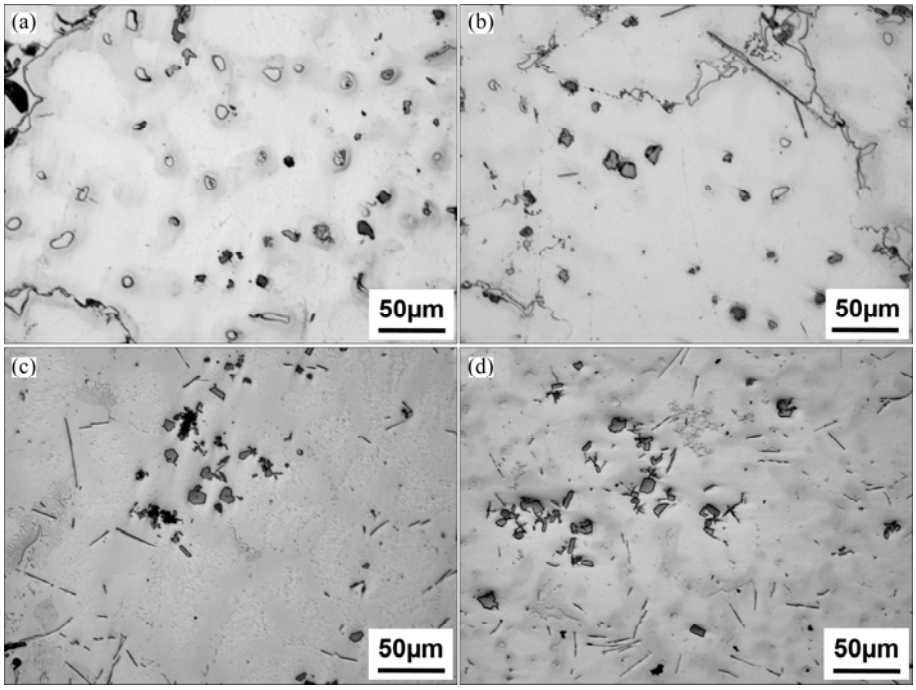

Fig. 6 Observation of Al_xNd_y precipitates distribution in as-cast AZ71 Mg alloys with different Nd additions: (a) 0.5%; (b) 1.0%; (c) 1.5%; (d) 2.0%

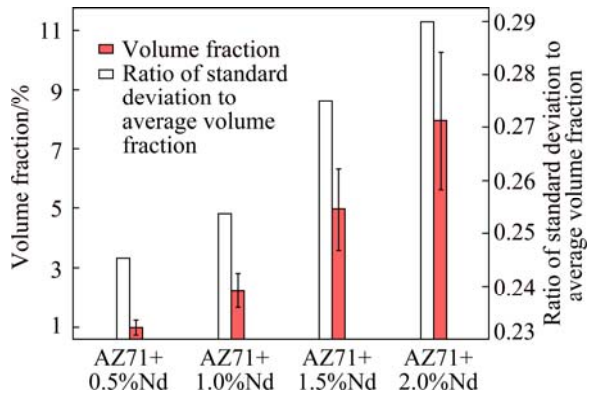

Fig. 7 Volume fraction of Al_xNd_y precipitates and ratio of their standard deviations to average volume fraction in as-cast AZ71 Mg alloys with different Nd additions

non-uniformly and aggregate with increasing the Nd addition. The aggregation of Al_xNd_y precipitates is especially prominent when the Nd addition exceeds 1.0%, as shown in Figs. 6(c), 6(d) and 7.

The optimal homogenization process was selected based on the full dissolution of β-$Mg_{17}Al_{12}$ phase and the breakdown of dendritic structures. Figure 8 demonstrates that the β-$Mg_{17}Al_{12}$ phase completely dissolves back into the matrix and forms equiaxed grains after homogenizing at 420 °C for 6 h. Heating at 420 °C for 6 h is thus chosen as the optimum homogenization treatment. It can be seen in Figs. 8(a_4), (b_4), (c_4), (d_4) and (e_4) that the Al_xNd_y precipitates still reside in the microstructures, because Al_xNd_y form at temperatures higher than the homogenization temperature.

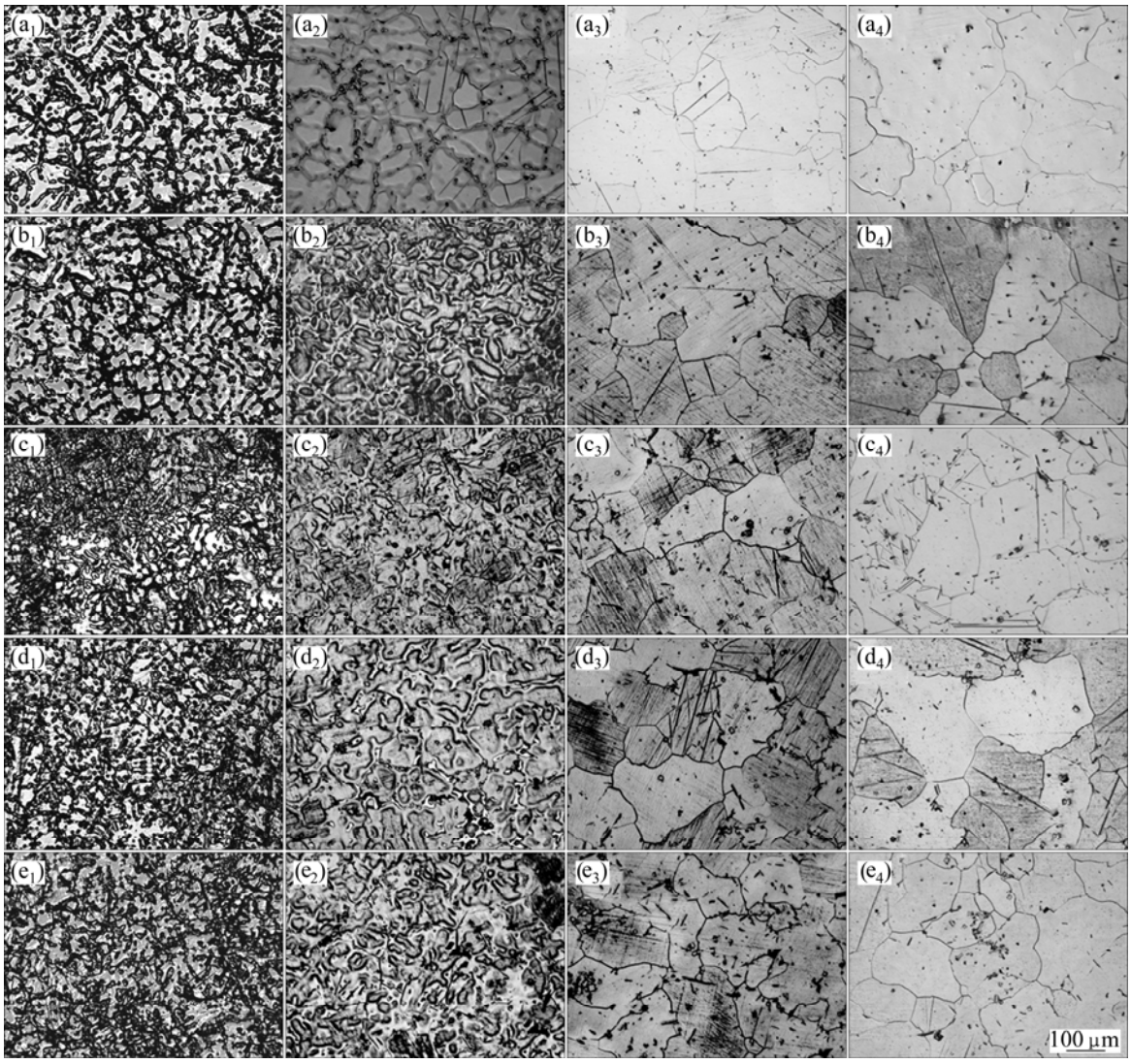

Fig. 8 Microstructures of AZ71 alloys with 0 (a_1−a_4), 0.5% (b_1−b_4), 1.0% (c_1−c_4), 1.5% (d_1−d_4), and 2.0% (e_1−e_4) Nd additions under as-cast (a_1, b_1, c_1, d_1, e_1), 300 °C homogenized (a_2, b_2, c_2, d_2, e_2), 380 °C homogenized (a_3, b_3, c_3, d_3, e_3), and 420 °C homogenized (a_4, b_4, c_4, d_4, e_4) conditions

3.2 Rotary forged and annealed structures

The homogenized AZ71 Mg alloys were subsequently rotary forged with 32% engineering strain at 200 °C. The extent of surface cracks decreases with increasing the Nd addition. No cracks are observed in the AZ71 Mg alloy containing over 1.0% Nd.

Figures 9(a_1), (b_1), (c_1), (d_1) and (e_1) show that the microstructures of rotary forged Mg alloy specimens consist of numerous twins and deformation bands. The density of defects increases with increasing the Nd content, obviously due to the nanosized Al_xNd_y precipitates. These fine precipitates are capable of pinning dislocation slips and distributing strains uniformly. The increase of twins and deformation bands increases the work hardening and thus higher uniform strains may be achieved in the Nd-added specimens. The accumulation of defects due to the Nd addition can also assist the dynamic recrystallization of AZ71 Mg alloy [23].

The rotary forged specimens subsequently underwent annealing processes at 200−350 °C for 1 h. The microstructures of rotary forged specimens annealed at 200 °C for 1 h are shown in Figs. 9(a_2), (b_2), (c_2), (d_2) and (e_2). Large amounts of plastic deformation and twin crystals are still present, with the widths of twins widened in comparison with those in Figs. 9(a_1), (b_1), (c_1), (d_1) and (e_1). When the annealing temperature further increases to 250 °C, new grains start to form, as shown in Figs. 9(a_3), (b_3), (c_3), (d_3) and (e_3). With increasing the Nd content, the extent of recrystallization increases as well, due to higher defect density. All tested alloys complete recrystallization after annealing at 350 °C, as shown in Figs. 9(a_5), (b_5), (c_5), (d_5) and (e_5). The annealed grain size decreases greatly from 230−

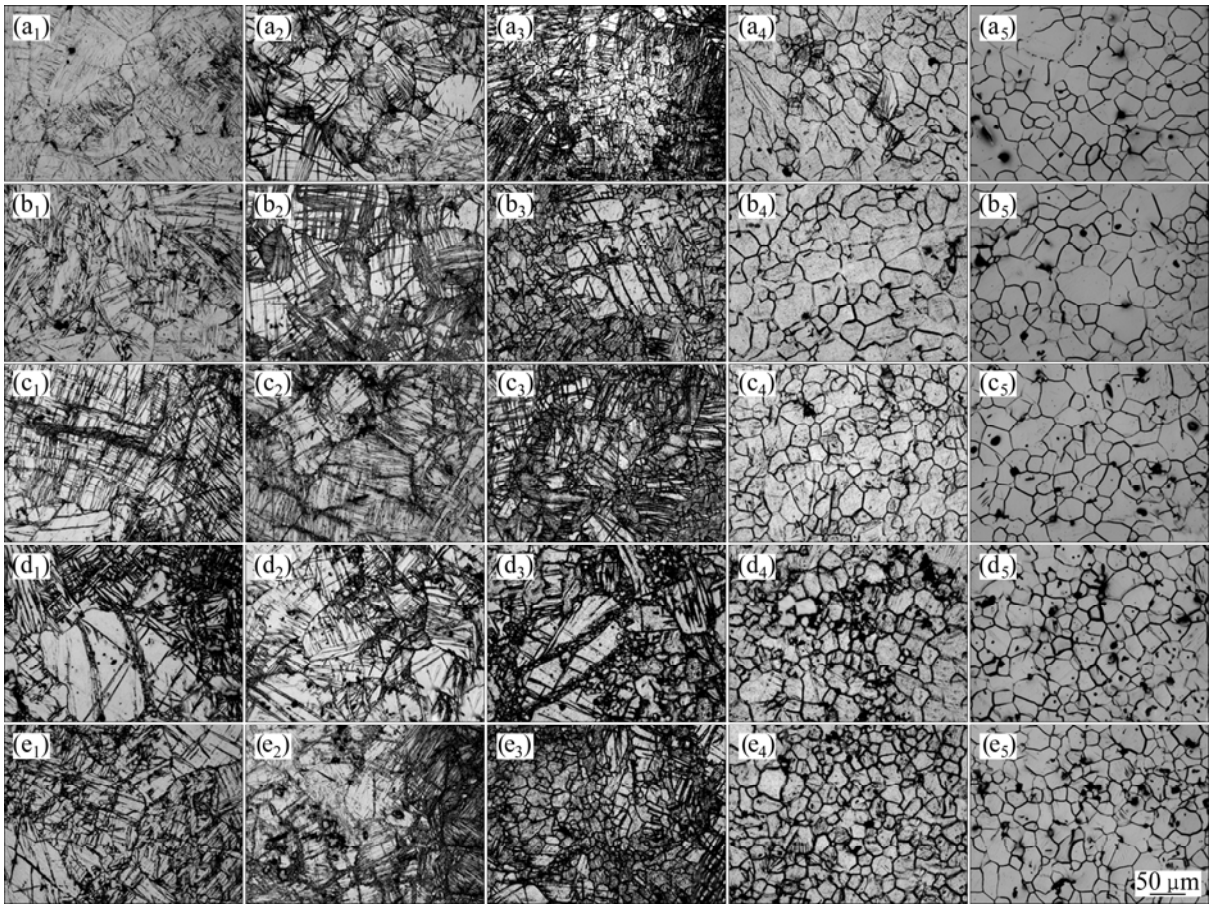

Fig. 9 Microstructures of AZ71 alloys with 0 (a_1−a_5), 0.5% (b_1−b_5), 1.0% (c_1−c_5), 1.5% (d_1−d_5), and 2.0% (e_1−e_5) Nd additions after rotary forging (a_1, b_1, c_1, d_1, e_1), and annealing at 200 °C (a_2, b_2, c_2, d_2, e_2), 250 °C (a_3, b_3, c_3, d_3, e_3), 300 °C (a_4, b_4, c_4, d_4, e_4), and 350 °C (a_5, b_5, c_5, d_5, e_5) for 1 h

365 μm under as-cast conditions to 21−50 μm (Fig. 2). Figure 2 demonstrates that the recrystallized grain size also reduces with increasing the Nd content.

For 1.0% Nd-added AZ71 Mg alloy, rotary forging and annealing processes decrease the grain size greatly from 241 μm of as-cast structures to 24 μm (Fig. 2). When over 1.0% Nd was added, the grain size does not decrease further, according to Figs. 2 and 9(c_5), (d_5) and (e_5). The 1.0% Nd addition to AZ71 Mg alloy is a critical content for grain refinement indicating that over-precipitation of Al_xNd_y can no longer aid to refine the grains.

In summary, the effects of Nd addition on the microstructures of AZ71 Mg alloy include multiple aspects: reducing the formation of β-$Mg_{17}Al_{12}$ and precipitating nanosized Al_xNd_y. The dissolved Nd in the matrix and nanosized precipitates assist to distribute the strain and defects uniformly, promoting grain refinement. However, when the precipitates aggregate, the grain size cannot further reduce.

3.3 Ambient mechanical properties

The tensile strength and elongation of the Nd-containing AZ71 Mg alloys are shown in Figs. 10 and 11, respectively. The tensile strength and ductility increase simultaneously with 0.5%−1.0% Nd addition in both as-cast specimens and forged-and-annealed specimens at room temperature. Both the strength and ductility reach the maximum values (253 MPa and 10.7%, respectively) by rotary forging and annealing 1.0% Nd-added AZ71 Mg alloy. Similar trends of maximum strength and elongation were observed as well in AZ81 Mg alloy with 2% Y and Nd addition by XIE et al [24]. Furthermore, according to Figs. 10 and 11, the standard deviations reduce greatly after rotary forging. A possible explanation is that the rotary forging process assists the reduction of casting porosity [17] and reduces the deviations in tensile tests.

The increase of strength in AZ71 Mg alloy with the Nd addition less than 1.0% can be attributed to the followings factors. 1) The Nd grain-refining effects increase the strength. 2) Nd contributes to both solution strengthening and precipitation strengthening. 3) The rotary forging and subsequent annealing further reduce the grain size and increase the strength. Nevertheless, the strength drops when the Nd addition exceeds 1.0% in

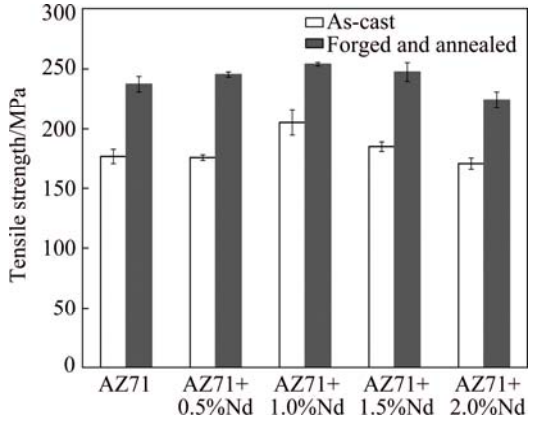

Fig. 10 Tensile strength of Nd-added AZ71 Mg alloys under as-cast condition and rotary forged and 350 °C annealed condition

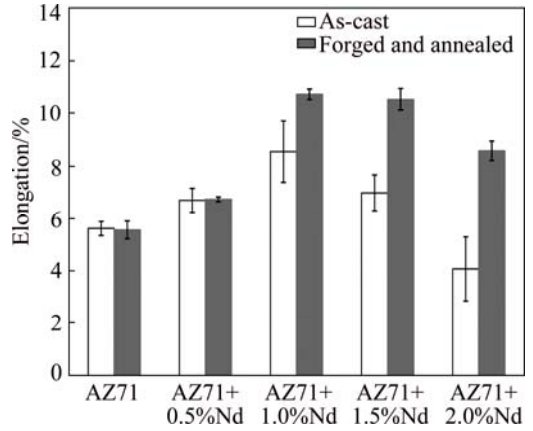

Fig. 11 Elongation of Nd-added AZ71 Mg alloys under as-cast condition and rotary forged and 350 °C annealed condition

AZ71 Mg alloy. For the AZ71 Mg alloy containing over 1.0% Nd, the aggregation of sharp rod-shape $Al_{11}Nd_7$ precipitates (Figs. 6(c) and (d)) acts as stress concentrators, reducing the strength.

On the other hand, Nd atoms are 13% larger than Mg atoms. The X-ray diffraction analyses (Table 2) show that the *c*/*a* ratio increases with increasing the Nd addition. This is in contrast to the Mg−Ce alloys where *c*/*a* does not change with increasing the Ce addition [9]. Because the ideal *c*/*a* ratio in hexagonal close packed structure is 1.633 ($\sqrt{8/3}$), the *c*/*a* ratio overpasses 1.633 when 1.5% or more Nd is added to AZ71 Mg alloy, according to Table 2. Larger *c*/*a* often implies that basal slip systems operate in preference to multiple slip systems [9].

However, according to Figs. 9(b_1), (c_1), (d_1) and (e_1), multiple orientations of deformation bands are observed in deformed grains indicating that multiple slip systems are operating. The large *c*/*a* ratio does not seem to restrict the operation of non-basal slip systems in the Nd-containing AZ71 Mg alloys. One possible reason is

Table 2 Effect of Nd addition on lattice parameters and *c*/*a* values of AZ71 Mg alloys

Alloy	$d_{(100)}$/nm	$d_{(101)}$/nm	*a*/nm	*c*/nm	*c*/*a*
AZ71	0.2781	0.2448	0.3211	0.5163	1.608
AZ71+ 0.5%Nd	0.2759	0.2437	0.3186	0.5191	1.629
AZ71+ 1.0%Nd	0.2753	0.2431	0.3185	0.5186	1.632
AZ71+ 1.5%Nd	0.2754	0.2433	0.3180	0.5199	1.635
AZ71+ 2.0%Nd	0.2741	0.2431	0.3168	0.5201	1.640

that the dissolved Nd atoms increase the critical resolved stress for basal slip. The increased stacking fault due to Nd addition also facilitates the ability of cross-slipping and allows slips other than basal system to operate [25]. The increase of slip systems thus contributes to the increase of ductility with the Nd addition up to 1.0%. The stress concentration effects of Al_xNd_y aggregate, on the other hand, cause the elongation to drop adversely when the Nd addition is over 1.0%.

4 Conclusions

1) The addition of Nd in AZ71 Mg alloy depresses the formation of β-$Mg_{17}Al_{12}$ eutectic phase and nanosized Al_xNd_y precipitates. The dissolved Nd in the matrix and nanosized Al_xNd_y precipitates aid to grain refinement which leads to the increase of strength and elongation at room temperature. When the Nd addition exceeds 1.0%, excess amount of Al_xNd_y precipitates aggregate and thereby deteriorate both strength and ductility.

2) The rotary forging process incorporated with annealing treatment significantly reduces the grain size from 230−365 μm under as-cast condition to 21−50 μm. The strength of 1.0% Nd-added AZ71 Mg alloy increases greatly from 177 MPa at as-cast state to 253 MPa after rotary forging and annealing. The elongation also increases significantly from 5.6% to 10.7%. The tensile strength of 253 MPa is comparable with that of AZ91 Mg alloy, while the elongation of 10.7% is amazingly 72% higher than that of commercial AZ91 Mg alloy. The addition of 1.0% Nd results in uniformly distributed nanosized Al_xNd_y precipitates and is the optimum concentration to be added in AZ71 Mg alloy.

Acknowledgments

This work was partly supported by the Ministry of Science and Technology of Taiwan under research grant No. MOST 103-2221-E-027-009 and Foxconn Technology Group.

References

[1] FROES F H, ELIZER D, AGHION E. The science, technology, and applications of magnesium [J]. JOM, 1998, 50(9): 30−34.

[2] CLOW B B. Magnesium industry overview [J]. Advanced Materials and Processes, 1996, 150(4): 33−34.

[3] DECKER R F. The renaissance in magnesium [J]. Advanced Materials and Processes, 1998, 154(3): 31−33.

[4] LI Y, CHEN Y, CUI H, XIONG B, ZHANG J. Microstructure and mechanical properties of spray-formed AZ91 magnesium alloy [J]. Materials Charaterization, 2009, 60: 240−245.

[5] ZHANG D, WANG S, QIU C, ZHANG W. Superplastic tensile behavior of a fine-grained AZ91 magnesium alloy prepared by friction stir processing [J]. Materials Science and Engineering A, 2012, 556: 100−106.

[6] XU Yan, HU Lian-xi, SUN Yu, JIA Jian-bo, JIANG Ju-fu, MA Qing-guo. Microstructure and mechanical properties of AZ61 magnesium alloy prepared by repetitive upsetting-extrusion [J]. Transactions of Nonferrous Metals Society of China, 2015, 25(2): 381−388.

[7] CHAPMAN J A, WILSON D V. Room-temperature ducitility of fine-grain magnesium [J]. Journal of the Institute of Metals, 1962, 91: 39−44.

[8] TIAN X, WANG L M, WANG J L, LIU Y B, AN J, CAO Z Y. The microstructure and mechanical properties of Mg−3Al−3RE alloys [J]. Journal of Alloys and Compounds, 2008, 465(1−2): 412−416.

[9] CHINO Y, KADO M, MABUCHI M. Enhancement of tensile ductility and stretch formability of magnesium by addition of 0.2 wt.%(0.035 at%) Ce [J]. Materials Science and Engineering A, 2008, 494(1−2): 343−349.

[10] MERLO F, FORNASINI M L. Volume effects in rare earth intermetallic compounds [J]. Journal of Alloys and Compounds, 1993, 197(2): 213−216.

[11] MAHMUDI R, KABIRIAN F, NEMATOLLAHI Z. Microstructural stability and high-temperature mechanical properties of AZ91 and AZ91+2RE magnesium alloys [J] Materials and Design, 2011, 32(5): 2583−2589.

[12] ZHANG J, WANG J, QIU X, ZHANG D, TIAN Z, NIU X, TANG D, MENG J. Effect of Nd on the microstructure, mechanical properties and corrosion behavior of die-cast Mg−4Al-based alloy [J]. Journal of Alloys and Compounds, 2008, 464(1−2): 556−564.

[13] WANG Ya-xiao, FU Jun-wei, YANG Yuan-sheng. Effect of Nd addition on microstructures and mechanical properties of AZ80 magnesium alloys [J]. Transactions of Nonferrous Metals Society of China, 2012, 22(6): 1322−1328.

[14] WANG Jing, SHI Bao-liang, YANG Yuan-sheng. Hot compression behavior and processing map of cast Mg−4Al−2Sn−Y−Nd alloy [J]. Transactions of Nonferrous Metals Society of China, 2014, 24(3): 626−631.

[15] OSAKADA K, GOTO Y, SHIRAISHI M, ODADA T. Shape control in CNC rotary swaging machine [J]. CIRP Annals–Manufacturing Techology, 1992, 41(1): 285−288.

[16] WANG Li-fei, HUANG Guang-sheng, LI Hong-cheng, ZHANG Hua. Influence of strain rate on microstructure and formability of AZ31B magnesium alloy sheets [J]. Transactions of Nonferrous Metals Society of China, 2013, 23(4): 916−922.

[17] GIRIBASKAR S, GOUTHAMA G, PRASAD R. Ultra-fine grained Al−SiC metal matrix composite by rotary swaging process [J]. Materials Science Forum, 2011, 702−703: 320−323.

[18] MANN R E D, HEXEMER R L Jr, DONALDSON I W, BISHOP D P. Hot deformation of an Al−Cu−Mg powder metallurgy alloy [J]. Materials Science and Engineering A, 2011, 528(16−17), 5476−5483.

[19] BISWAS S, SKET F, CHIUMENTI M, GUITIERREZ-URRUTIA I, MOLINA-ALDAREGUIA J M, PEREZ-PRADO M T. Relationship between the 3D porosity and β-phase distributions and the mechanical properties of a high pressure die cast AZ91 Mg [J]. Metallurgical and Materials Transactions A, 2013, 44(9): 4391−4403.

[20] ASTM E8/E8M. Standard test methods for tension testing of metallic materials [S].

[21] LIU H, CHEN Y, TANG Y, HUANG D, NIU G. The microstructure and mechanical properties of permanent-mould cast Mg−5wt%Sn−(0−2.6) wt%Di alloys [J]. Materials Science and Engineering A, 2006, 437(2): 348−355.

[22] ZHANG J, WANG Z, SUN W, ZHU M. Microstructure and corrosion behavior of AZ91−0.4%Nd magnesium alloy [J]. Applied Mechanics and Materials, 2013, 291−294: 2577−2580.

[23] YANG X, MIURA H, SAKAI T. Dynamic evolution of new grains in magnesium alloy AZ31 during hot deformation [J]. Materials Transactions, 2003, 44(1): 197−203.

[24] XIE Jian-chang, LI Quan-an, WANG Xiao-qiang, LI Jian-hong. Microstructure and mechanical properties of AZ81 magnesium alloy with Y and Nd elements [J]. Transactions of Nonferrous Metals Society of China, 2008, 18(2): 303−308.

[25] CHINO Y, KADO M, MABUCHI M. Compressive deformation behavior at room temperature−773 K in Mg−0.2 mass% (0.035 at.%) Ce alloy [J]. Acta Materialia, 2008, 56(3): 387−394.

钕与旋锻对 AZ71 镁合金力学性能的影响

陈贞光[1]，陈宇辰[1]，李宪宗[2]，陈锦修[2]，张浚荣[2]

1. 国立台北科技大学 材料科学与工程研究所，台北市 10608；2. 鸿准精密工业股份有限公司，新北市 23680

摘 要：探讨钕的添加对 AZ71 镁合金的力学性能和塑性加工性能的影响。添加 0.5%~2.0%的钕时，AZ71 镁合金的晶粒尺寸和脆性 β-$Mg_{17}Al_{12}$ 相的含量均随着钕添加量的增加而降低，并形成纳米级的 Al_xNd_y 析出相。经过 32%旋锻和退火后，加钕 AZ71 镁合金的晶粒尺寸由 350 μm 减小到 30 μm 以下。当钕的添加量达到 1%时，合金的强度与延性可同时获得提升；当钕的添加量超过 1%时，组织中杆状 $Al_{11}Nd_3$ 以及块状 Al_2Nd 聚集析出，导致合金的强度与延性降低。因此，1.0%钕添加量为 AZ71 镁合金的最佳添加量，添加 1.0%钕的 AZ71 镁合金可以获得 253 MPa 的抗拉强度和 10.7%的伸长率，在铸态或经旋锻退火后均具有最高的韧性。

关键词：AZ71 镁合金；钕；旋锻；力学性能；再结晶

(Edited by Mu-lan QIN)